Earth Systems and Environment (2019) 3:277–288
https://doi.org/10.1007/s41748-019-00106-z

ORIGINAL ARTICLE

# Identifying Agricultural Systems Using SVM Classification Approach Based on Phenological Metrics in a Semi-arid Region of Morocco

Y. Lebrini[1,3] · A. Boudhar[1,2] · R. Hadria[3] · H. Lionboui[3] · L. Elmansouri[4] · R. Arrach[5] · P. Ceccato[6] · T. Benabdelouahab[3]

Received: 20 April 2019 / Accepted: 21 June 2019 / Published online: 29 June 2019


**Abstract**
To understand changes in agricultural systems, it is necessary to monitor vegetation dynamics based on the spatio-temporal characterization of phenological parameters. The purpose of this study is to identify the main agricultural systems using a phenology-based classification method in a semi-arid context. Phenological metrics were derived from Normalized Difference Vegetation Index time series extracted from MOD13Q1 product between 2012 and 2016. Furthermore, Support Vector Machine classification method was applied based on phenological metrics, to identify the main agricultural system classes in the study area. The main classes are; (1) irrigated annual crop, (2) irrigated perennial crop, (3) rainfed area and (4) fallow. The classification overall accuracy reached 88%, with a kappa coefficient of 0.83 and values of $F1$-score greater than 0.76. The results demonstrated the ability of phenological parameters to identify and monitor the main agricultural system classes in the study area and to control the illegal pumping zones.

**Keywords** Phenological metrics · Agricultural systems · SVM · Semi-arid · MODIS

## 1 Introduction

In arid and semi-arid regions, the effects of climate change can be dramatic on agriculture whose production depends largely on the quantity and distribution of annual rainfalls (Almazroui et al. 2017b; DeFries et al. 1999; Dixon et al. 1994). The global changes in land cover are at the origin of the disturbances observed in the agricultural cycle.

✉ Y. Lebrini
y.lebrini@usms.ma

1 Water Resources Management and Valorisation and Remote Sensing Team, Faculty of Sciences and Techniques, Sultan Moulay Slimane University, Beni Mellal, Morocco

2 Center for Remote Sensing Application (CRSA), Mohammed VI Polytechnic University, Ben Guerir, Morocco

3 National Institute of Agronomic Research, Rabat, Morocco

4 Agronomic and Veterinary Institute Hassan II, Rabat, Morocco

5 Ministry of Agriculture, Fisheries, Rural Development, Water and Forests, Direction of Strategy and Statistics, Rabat, Morocco

6 International Research Institute for Climate and Society, The Earth Institute, Columbia University, New York, USA

In the semi-arid context, successive droughts and floods affect the land cover and the socio-economic development, especially in arid and semi-arid regions (Almazroui et al. 2017a; Barakat et al. 2019; Lionboui et al. 2014). In these areas, agricultural production depends on the spatio-temporal distribution of the rainfall amount (Benabdelouahab et al. 2016; René and Nathalie 2007). Hence, evaluating and monitoring land cover is an essential element for global changes (DeFries et al. 1999; Jung et al. 2006; Lambin et al. 2001).

The monitoring of vegetation cover variability during agricultural seasons allows managers and policy makers to manage agricultural systems (Löw et al. 2013). In this context, remote sensing can provide essential tools to support large-scale agricultural monitoring systems through vegetation indices. Many studies affirmed that vegetation indices used to produce phenological parameters based on time series data provide accurate and robust classification results compared to traditional methods that use a single image (Alcantara et al. 2012; Pal and Mather 2005).

Phenological parameters provide information on plants' periodicity, as well as the monitoring of the appearance and occurrence of phenological events, such as onset, senescence, length of season and peak of biomass production (Lieth 1974; Schmidt et al. 2015; Schwartz 2003). Remote sensing time series analysis based on Normalized Difference Vegetation Index (NDVI) can be one of the most reliable tools for mapping and characterizing the vegetative development behaviors among cropping seasons.

Many studies used phenological parameters extracted along one or several seasons in different applications: (i) for crop mapping (Arvor et al. 2011; Lessel and Ceccato 2016; Wardlow et al. 2007), (ii) crop yield and agricultural production (Mottaleb et al. 2015; Shahriar et al. 2014; Zhao et al. 2017), (iii) analyzing the spatio-temporal trends of the vegetation linked to climate (Evrendilek and Gulbeyaz 2011; Peng et al. 2013; Vrieling et al. 2011), (iv) extracting pheno-regions and biomass quantification (Diouf et al. 2014, 2015) and monitoring drought dynamics effects on agriculture (McVicar and Jupp 1998; Winkler et al. 2017; Wu et al. 2015).

Phenological observations (e.g., biomass accumulation, peak of greenness, and period of leaf development) in agriculture provide valuable information to improve yield prediction models (Hadria et al. 2006, 2007; Viña et al. 2004). Therefore, it is important to be able to monitor and determine accurately the spatio-temporal variability of phenological metrics (e.g., length, start, and end of the agricultural season) and to analyze their behavior in arid and semi-arid regions. This study is crucial in filling the gap of information to monitor agricultural area using phenological metrics and to help managers and decision makers to analyze the agricultural policies' impact and to optimize the land use choices.

The aim of the present study is twofold: (1) spatio-temporal analysis of phenological parameters patterns using four seasons of NDVI time series obtained from MODIS satellite data, (2) map the main phenological classes through phenology-based classification approach.

## 2 Data and Methodology

### 2.1 Data

#### 2.1.1 Study Area

The study area is covered by Moderate Resolution Imaging Spector-radiometer (MODIS), tile: h17v05, clipped to Beni-Mellal-Khenifra region located in centre of Morocco, with a total area of 28,374 km$^2$ that represent about 4% of the national territory (Fig. 1). In the geomorphological aspect the region includes four geographical units; the Atlas Mountains, the foothill area that represents the transition between the Mountain and the Tadla plain, the phosphate plateau and the irrigated perimeter of Tadla. The study area topography

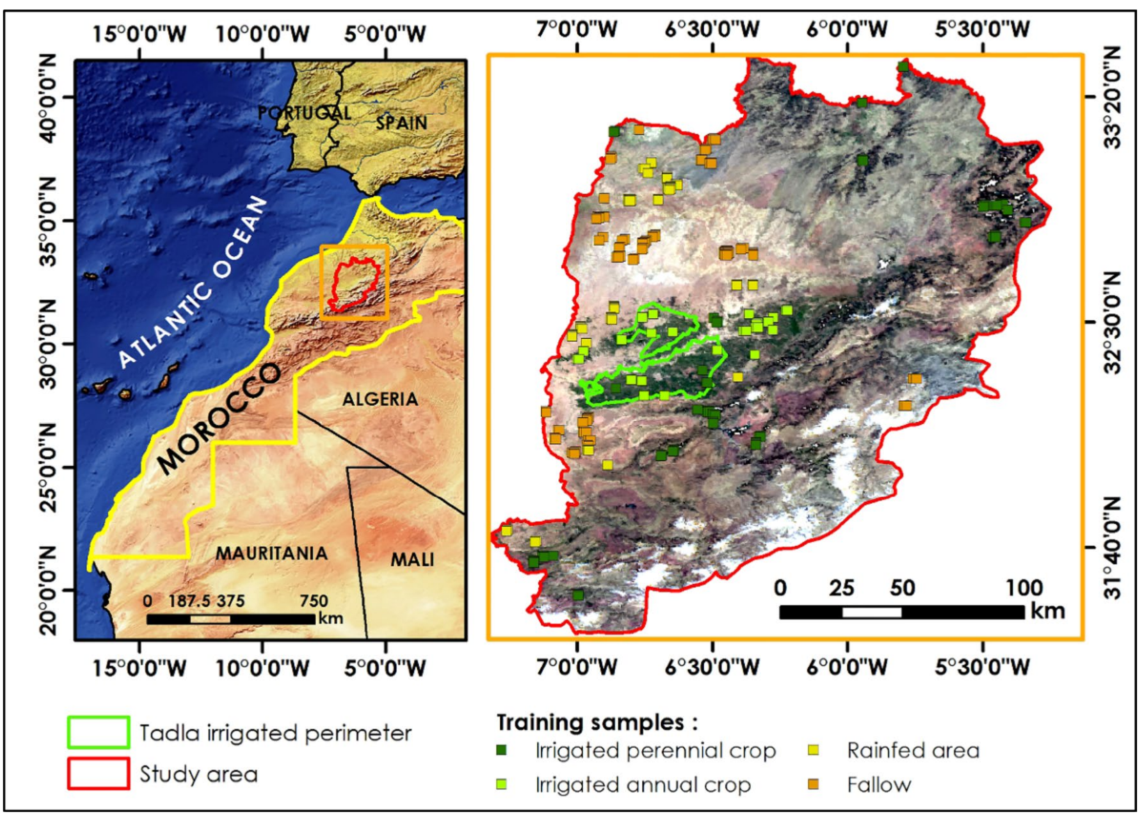


**Fig. 1** Localisation of the Beni-Mellal-Khenifra region and the training samples

ranges from 300 m above sea level, in the plan to 3890 m in the Mountain. About half the region is Mountainous (from 900 to 3890 m) while the other half consists of plains and plateaus (around 600 m).

The main agricultural classes present in this region are the irrigated perimeter, the rainfed area (no irrigated), the fallow, and the foothill zone (trees and forest). Climate is variable from humid in the high mountains to semi-arid in the plain, with an intense cold winter and very hot summers. In addition, the annual average rainfall is characterized by significant variations, with a rainfall average amount of 230 mm in the plain and 1000 mm in the high mountains (Marchane et al. 2015; Ouatiki et al. 2019). The average annual temperatures vary between a maximum of 46 °C in August and a minimum of − 2 °C in January (Ouatiki et al. 2017).

The agricultural sector is one of the most promising sectors in the region and constitutes the main economic activity. The useful agricultural area in the region is about 948,397 ha of which 212,000 ha is irrigated (CRI 2015). The region is characterized by a large irrigation scheme covering about 100,000 ha and a small and medium hydraulic zone (foothill area) with an approximate surface area of 81,787 ha (Lionboui et al. 2016).

#### 2.1.2 Satellite Data

Moderate Resolution Imaging Spectro-radiometer (MODIS) was used to characterize the spatio-temporal dynamics of phenological metrics (Fig. 3). A set of 92 images of MOD13Q1 16-day composites product at 250 m resolution covering the study area has been acquired between 2012 and 2016 (23 images per year). All images have been downloaded through the United States Geological Survey (USGS) reverb tool (NASA LP DAAC). MOD13Q1 product is calculated from the Level-2G daily surface reflectance gridded data (MOD09 and MYD09 8-day composites series) using the Constrained View angle-Maximum Value Composite method (CV-MVC) (Didan 2015). MODIS-Terra is a near-polar orbiting satellite operated by NASA and has many spectral bands, NDVI, EVI, Bleu, NIR, Red, MIR and quality bands (Didan 2015). For the overall studied seasons, NDVI layers were used to produce NDVI time series.

In this study, the NDVI index was used for monitoring phenological parameters. This choice is based on the sensitivity of this index to vegetation canopy variations in areas characterized by a low plant density, unlike other indices such as EVI (Enhanced Vegetation Index) (Ji and Peters 2007). The study concerns different agricultural production units with low (fallow), medium (rainfed) and high (irrigated area) crop density and growth potential. Normalization methods is another advantage of this index, which allows the minimization of shadow effects, noise related to the atmospheric conditions and the solar angle change (Matsushita et al. 2007). NDVI takes advantage of the degree of absorption by chlorophyll in the red and the scattering of leaves in the near infrared radiation of which is proportional to vegetative development (Tucker et al. 1983).

The land cover map originated from Glob Cover (Hadria et al. 2018; Kaptué et al. 2011), served as a mask for the agricultural zones in the study area. This map was developed by the Flemish Institute for Technological Research, Belgium (VITO), in the E-AGRI project (http://www.e-agri.info).

#### 2.1.3 Training Site

We selected four land cover types: irrigated perennial crop, irrigated annual crop, rainfed area and fallow, to evaluate the effectiveness of the curve fit for remotely sensed NDVI data within the Beni-Mellal-Khenifra Region. Agricultural systems' types zones were identified and selected in 2016 and are distributed across the study area (Fig. 1). For the period from 2012 to 2016, a verification step was carried out using ground truth data from field survey and Google Earth to confirm the no-change of the agricultural system type. Type localities consist of 40 irrigated annual crop locations containing 210 pixels, 40 irrigated perennial crop locations containing 301 pixels, 40 rainfed crop locations containing a total pixels of 254 and 40 fallow locations containing a total of 441 pixels (Table 1). Time series of an arbitrarily selected pixel from each land cover type are shown in Fig. 1.

Irrigated annual crop represents a high degree of interannual variability with a high amplitude and abrupt growth and senescence. The irrigated perennial crop was selected as representative of a high base and weak amplitude. Rainfed crop and fallow were selected as representative of typical semi-arid land cover, which depends on climate conditions and may not have a pronounced phenology.

**Table 1** Classes and size of the training data set

| Class name | Number of training samples (pixel) |
|---|---|
| Irrigated annual crop | 210 |
| Irrigated perennial crop | 301 |
| Rainfed area | 254 |
| Fallow | 441 |
| Total | 1206 |

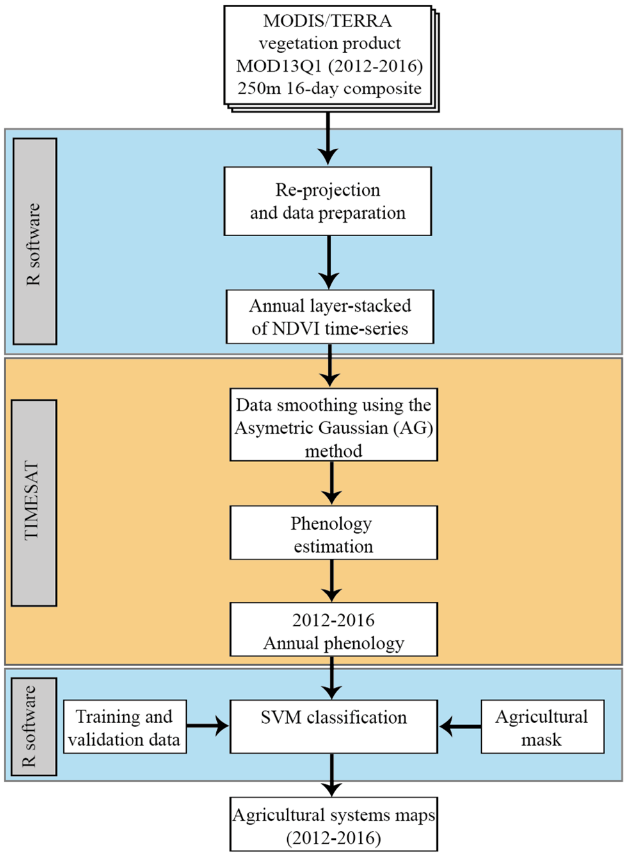


**Fig. 2** Schematic diagram illustrating the research methodology adopted in this study

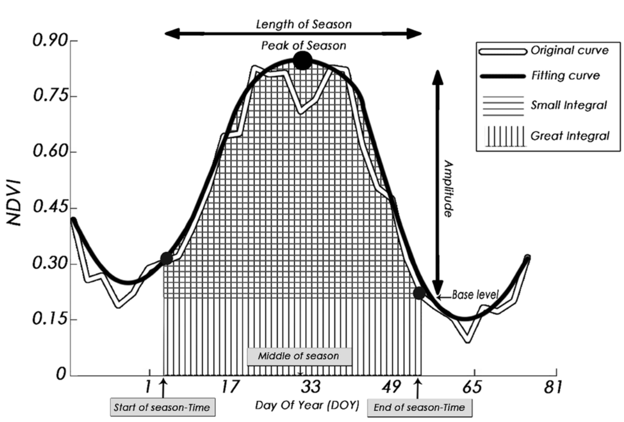


**Fig. 3** Phenological parameters available in TIMESAT software. Adapted from Jönsson and Eklundh (2004)

## 2.2 Methodology

Three steps were carried out to map agricultural systems over the study area using phenological metrics extracted from the NDVI time-series data (Fig. 2).

### 2.2.1 Data Time Series Analysis

To analyze and extract phonological metrics (Fig. 3 and Table 2) NDVI time series profiles were generated from 2012 to 2016, using TIMESAT Program (Fig. 3). TIMESAT software was developed by Eklundh and Jönsson (2015) and it was used for estimating seasonal phenological metrics (Table 2). TIMESAT implements three processing methods using a preliminary definition of the seasonality (unimodal or bi-modal) with approximations of growing season times. These methods are Savitzky-Golay (SG) (Chen et al. 2004), Gaussian asymmetric (GA) (Bachoo and Archibald 2007; Chen et al. 2006) and double logistic (DL) (Geng et al. 2014), which require several statistical parameters of adjustment.

The GA and DL approaches seem to be less sensitive to noise than the SG approach (Jönsson and Eklundh 2002, 2004). In this study, the GA filter was used for its low sensitivity to noise and high ability to process the satellite data series. The phenological metrics values were extracted for the sampled pixels. These values were analyzed using a statistical method to display the distribution of data based on the extremes, first quartile, median and third quartile (boxplot) (McGill et al. 1978). The boxplots help to make comparisons across phenological parameters to analyze the behavior of the phenological metrics in terms of agricultural systems.

### 2.2.2 Classification of Time-Series Data

In this study, Support Vector Machine (SVM), which is a supervised nonparametric statistical technique, was used as a classification method. SVM is a mathematical technique for solving the classification problems with a high generalization capability from small training samples and a high potentiality for regional characterization study (Shao and Lunetta 2012; Vapnik 2006). The open-source R language and software was used to implement the SVM classification using the "CARET" package (Jed Wing et al. 2018; R Core Team 2017). Four classes were considered, namely irrigated annual crop, irrigated perennial crop, rainfed area and fallow (Fig. 4). The accuracy assessment was carried out using overall accuracy, producer and user accuracy, $F1$ score and the Kappa coefficient.

SVM with Radial Basis Function (RBF) kernel was used due to this robustness and effectiveness for remote sensing data classification (Mountrakis et al. 2011). Defining Kernel function parameters (g and C) is required to use the SVM method. The optimal choice of these parameters was performed using the "CARET" package. The tuning step was performed based on 2015/2016 data. Then, the optimal model was defined and used to classify the agricultural systems over the study area.

**Table 2** Definition of computed phenological parameters (Eklundh and Jönsson 2015; Reed et al. 1994)

| Phenological metric | Phenological definition |
|---|---|
| Start of season—time | Beginning of photosynthesis activity in the vegetation canopy |
| End of season—time | End of photosynthesis activity in the vegetation canopy |
| Length of season (LOS) | Length of photosynthetic activity |
| Peak of season | Maximum level of photosynthetic activity |
| Middle of season | Mean value of the times for which left edge increases to 80% and right edge decreases to 80% |
| Great integral (GINT) | Canopy photosynthetic activity across the entire growing season |
| Small integral (SINT) | Canopy photosynthetic activity between the function describing the season and the base level |
| Amplitude | Maximum increase in canopy photosynthetic activity above the baseline |
| Base level | The average of the left and the right minimum values |

## 3 Results and Discussion

### 3.1 NDVI Profile Analysis

In this step, NDVI profile responses were represented in Fig. 4 at the pixel-level in the time-series MODIS data for each agricultural system class which are; the irrigated perennial crop (Fig. 4a), the irrigated annual crop (Fig. 4b), the rainfed area (Fig. 4c) and the Fallow (Fig. 4d). The multi-temporal NDVI profile of a specific agricultural system reflects its phenological characteristics (e.g., start, end, and length of season).

Figure 4 shows four different categories of profiles, which are characterized by a well-defined shape. For each category, the phenological metrics values depend on the NDVI profile size and dimensions. Figure 4a, b is discriminated by their high values of the NDVI peak ranges from 0.7 to 0.9, unlike that for Fig. 4d and partially for Fig. 4c. The NDVI profile in Fig. 4a is characterized by its high base value, which indicates a perennial crop zone with high and permanent photosynthetic activity. The opposed profiles observed in IPC agricultural system were originated from the phenological cycle of certain irrigated perennial crops (e.g., pomegranate), which starts the photosynthetic activity in late March and reach the maximum on around June (Fig. 4a). The length of the cropping season (LOS) lasts longer for Fig. 4a, b where the season length takes more than 8 months, in contrast to other two profiles where LOS takes less than 5 months.

NDVI profiles for the rainfed area (Fig. 4c), and fallow (Fig. 4d) show an important internal variability linked to the cropping season climate conditions. Accordingly, all phenological parameters in these areas are directly influenced by the local climate fluctuations; mainly the water amount available from rainfall events over each season.

Regarding the start of season criteria, NDVI values in irrigated zones are heterogeneous (Fig. 4a, b). This observed

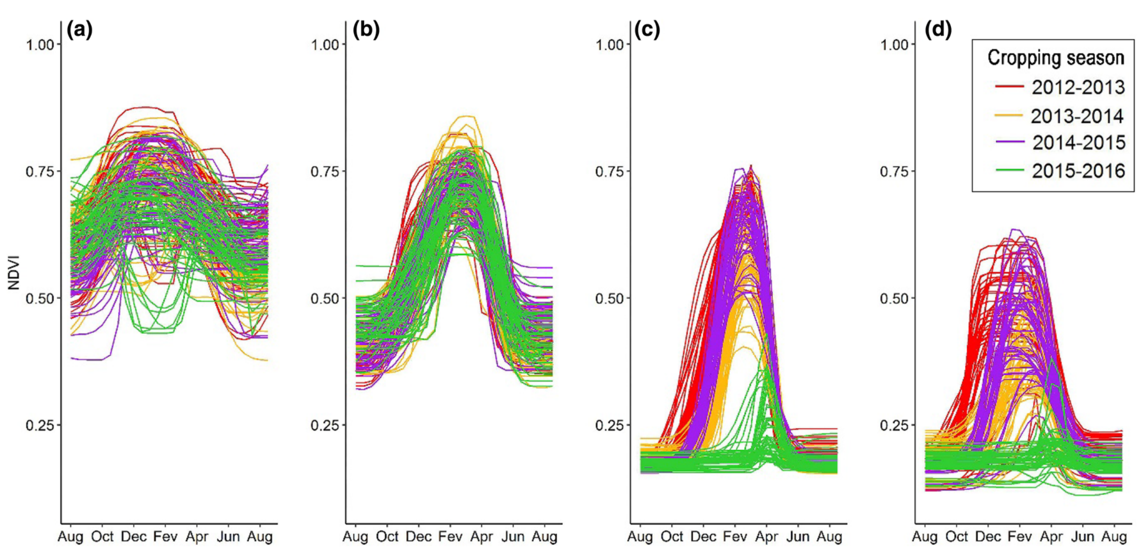


**Fig. 4** NDVI profiles for land surface phenology in the study area. **a** Irrigated perennial crop, **b** irrigated annual crop, **c** rainfed area, **d** fallow

heterogeneity is due to the farmer decision about sowing dates and the irrigation water supplies moments. Adversely, the start of season in the rainfed area, as shown in Fig. 4c, d, is homogeneous due to the crop dependence to the first rainfall event. For the amplitude parameter, as shown in Fig. 4a, b, irrigated perennial crop zones are characterized by lowest amplitude values, contrary, highest amplitude values are observed in the irrigated annual crops profile.

## 3.2 Phenological Parameters Analysis

The phenological metrics were computed for each pixel on the basis of the NDVI profile. The distribution of these metrics was analyzed using boxplot representation to study their behavior regarding the agricultural system classes. Figure 5a, b, f–h represents statistics of the studied phenological metrics for each phenological classes. The amplitude and small integral metrics confound irrigated perennial crops and fallow (Fig. 5a, g). Similarly, the rainfed area and fallow classes are not separable when just using the base level and the end-of-season metrics (Fig. 5b). The middle of season and the end of season confounded between the irrigated annual crops, rainfed area and fallow (Fig. 5f, h).

Unlike previously cited indicators, the great integral, the start of season, the peak and the length of the season parameters provide valuable information to discriminate between surface classes (Fig. 5c–e, i). Based on these results, we focused on the spatial analysis of the phenological metrics for the 2015/2016 season (Fig. 6).

The parameters showed high spatial variability and a contrasting level of phenological responses. Indeed, according to Jönsson and Eklundh (2002), the great integral (GINT) indicates the level of plant biomass production. This production is strongly related to water availability in the arid and semi-arid areas (Benabdelouahab et al. 2015). Similarly, in the irrigated area (irrigated and pumping zone) the length of the season (LOS) parameter takes a longer period compared to the non-irrigated area due to the irrigation water supplies during the critical periods of crop development (Figs. 4, 6). Since the LOS parameter was calculated based on the difference between the end (Fig. 6h) and the start of the cropping season (Fig. 6c), it plays a key role to observe the length of the biomass production period.

For the case of irrigated area of the studied zone (Tadla irrigated perimeter, foothill area, and pumping area), the values of GINT, LOS, and the Base level are high and range

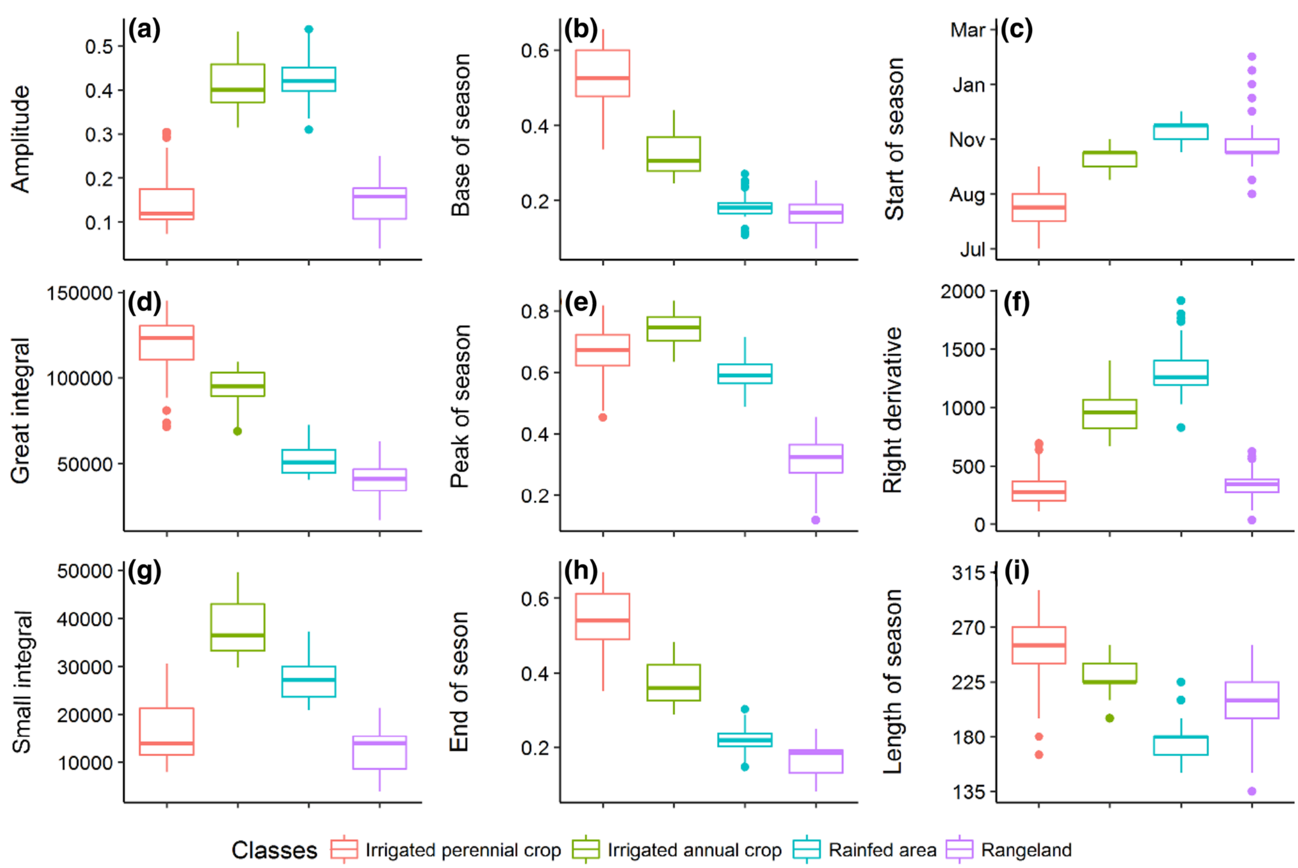


**Fig. 5** Boxplot presenting the phenological parameters behavior in the study area

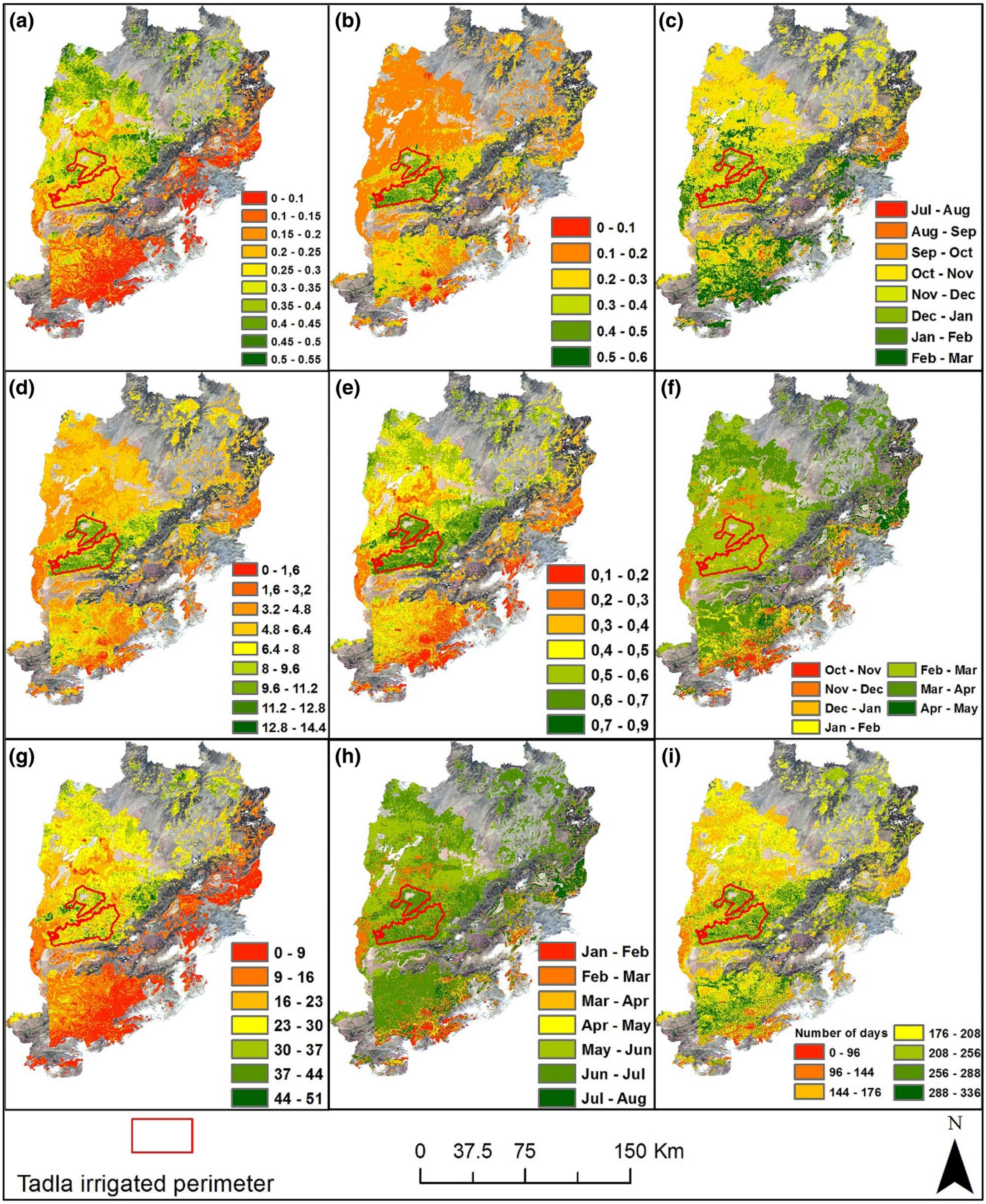


**Fig. 6** Seasonality maps of the nine phenological parameters: **a** amplitude, **b** base, **c** end of season, **d** great integral, **e** peak, **f** middle, **g** small integral, **h** end of season, **i** length of season. The background is a RGB composite of MODIS image

from 11.2 to 14.4, 256 to 288 days and from 0.4 to 0.6, respectively (Fig. 6b, d, i). The peak of season parameter indicates the highest level of NDVI values in the irrigated area with values ranging between 0.6 and 0.9 (Fig. 6e). Adversely, the rainfed area and fallow zones are characterized by the lowest GINT, LOS, and peak values with less than 6.4, 208 days and 0.4, respectively, but are more distinguished by amplitude and middle-of-season metrics (Fig. 6a, f). Regarding the short integral metrics (SINT), the high values observed correspond to the perennial crops characterized by high biomass production during the cropping season (Fig. 6g). As seen by these results, phenological parameters values in the rainfed area and fallow zones depend on the cropping season climate conditions. The nine phenological parameters are considered as keys parameters to discriminate the different phenological zones (Fig. 6).

### 3.3 SVM Classification

The specific objective of this step is to classify, at the overall study zone, the discriminated area combining the nine phenological parameters, discussed previously, as input to the SVM classifier. The optimal model was selected based on the tuning step of the classifier since it ensures the highest accuracy ($C=8$ and $g=0.274$). To evaluate the accuracy of the classification, a confusion matrix was established by comparing classification results with reference data essentially based on ground truth data (Table 3).

The confusion matrix results are 88.7% and 0.83 for overall accuracy and kappa coefficients, respectively. For the irrigated annual crop class, it was accurately classified with 92.59% and 86.21% for producer and user accuracy, respectively (Table 3). Concerning the irrigated perennial crop class, it was mapped correctly with 92.98% of producer accuracy that has been ranked correctly considering the reference data and user accuracy of 94.64% that has been mapped with the classification algorithm (Table 3). For this class, about 6% of the pixels were committed to other classes. Producer accuracy for the Rainfed area class is about 81.25%, as long as it is about 88.64% for the user accuracy, i.e., 11.36% of the rainfed area class have been classified inaccurately (Table 3). Rainfall area class results show a high omission error value of around 0.18. This is justified by the behavior of rainfed crops in relation to the climatic conditions of the agricultural season. An extremely dry year will condition the rainfall area to behave as a fallow area. Contrary to the good climatic conditions, which allow the rainfed areas to have a phenological behavior relatively similar to the irrigated crops. The fallow class has accuracy values of 91.30% and 88.42% for the producer and user accuracy, respectively (Table 3).

Phenological parameters extracted in this study showed high spatio-temporal heterogeneity over the study area. The contrasting differences between the derived parameters could be explained by the complex relationship between the rainfall anomalies and vegetation cover. The heterogeneous behavior of the vegetation cover is also influenced by climatic conditions, natural resources availability and land-use practices such as rainfall amount and distribution, amount of irrigation water supply and access mode, soil quality and technical itinerary (Benabdelouahab et al. 2016).

The obtained classification results for the 2014/2015 cropping season were compared to the official statistics from the Regional Investment Centre (CRI) to assess the ability of the proposed classification method to predict the agricultural system superficies over the region (CRI 2015) (Figs. 7, 8).

The total irrigated class superficies is about 414,081 ha compared to 212,000 ha of the irrigated area estimated by CRI (CRI 2015). This gap is due essentially to the no-controlled pumping area that is not involved in the official statistics. The pumping area can be detected and estimated using the developed classification approach based on phenological remotely sensed data. This approach constitutes a relevant way, for local policy makers and managers, to monitor and control the irrigated and the rainfed agricultural zones (Lionboui et al. 2016).

Furthermore, superficies estimation errors can be also related to the low resolution of the MOD13Q1 data product used in this study. In this case, one pixel can represent a mixture of two classes or more due to the short cover type change (Biggs et al. 2006; Boschetti et al. 2009). The dominant class will be retained, given its influence on the phenological behavior for each pixel (Sun et al. 2012).

**Table 3** Confusion matrix obtained from the SVM classifier for the 2015/2016 agricultural season

| Class | Producer accuracy (%) | User accuracy (%) | $F1$ score | Commission error | Omission error |
|---|---|---|---|---|---|
| Fallow | 91.3 | 88.42 | 0.88 | 0.08 | 0.09 |
| Irrigated annual crop | 92.59 | 86.21 | 0.91 | 0.02 | 0.07 |
| Irrigated perennial crop | 92.98 | 94.64 | 0.95 | 0.02 | 0.07 |
| Rainfed area | 81.25 | 88.64 | 0.77 | 0.03 | 0.19 |
| Overall accuracy | 88.7 | | | | |
| Kappa coefficient | 0.83 | | | | |

**Fig. 7** Classification results of the agricultural system classes. The background is a RGB composite of MODIS image

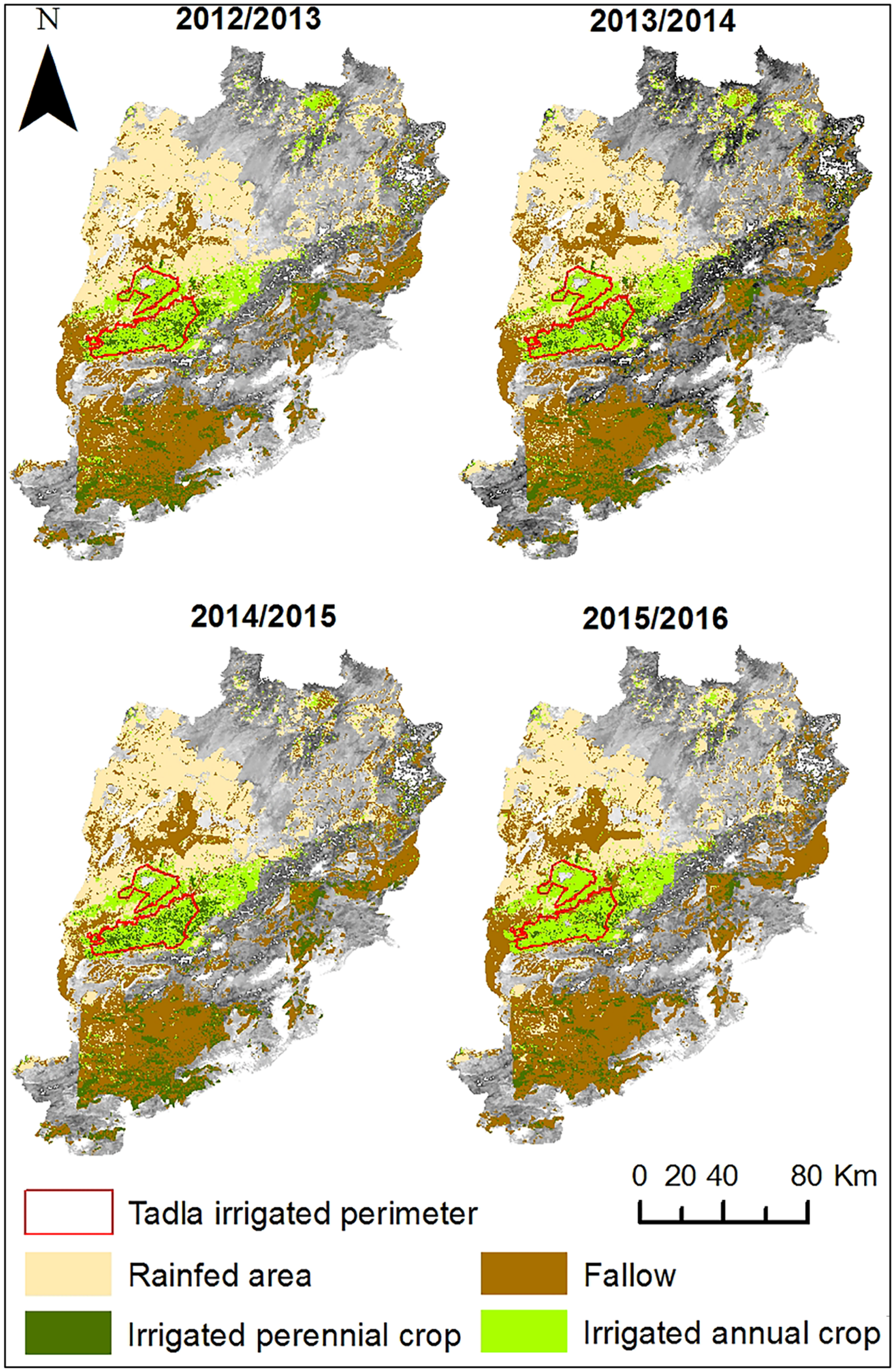


Concerning the change in agricultural superficies, the fallow class has raised from 1,256,000 ha in 2014/2015 to 1,506,000 ha in the 2015/2016 cropping season (Fig. 8). The increase of fallow superficies observed in the 2013/2014 (1,308,682 ha) and 2015/2016 (1,505,873 ha) cropping seasons is strongly related to rainfall with an average amount of 232 mm and 128 mm, respectively. Adversely, the fallow superficies are less than 1,260,000 ha, i.e., 2012/2013 and 2014/2015 cropping seasons, with an average amount of rainfall higher than 380 mm (Fig. 8). For the same reason, the rainfed class area has decreased and classified as fallow area due to the lack of rainfall during the 2015/2016 cropping season. Irrigated areas are partially independent of climatic conditions. Except for the extremely dry years

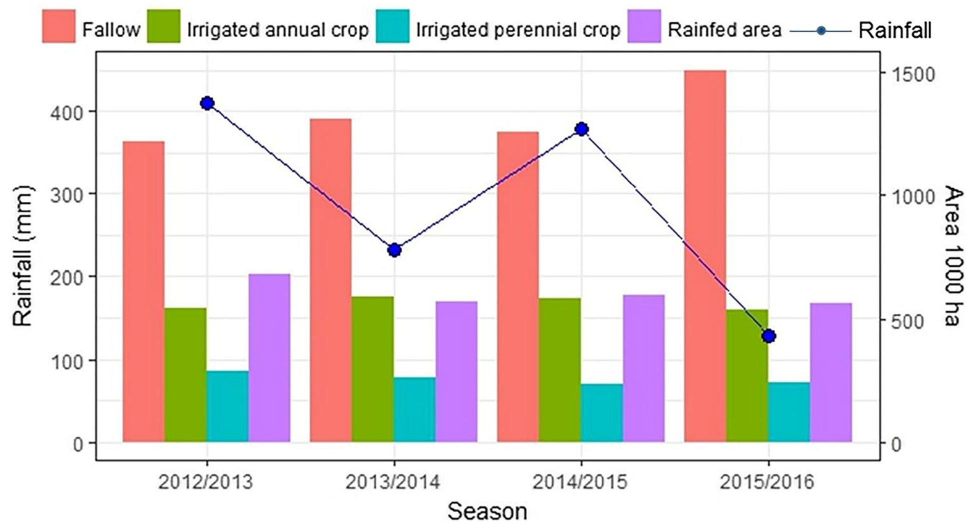


**Fig. 8** Area of phenological classes predicted by the SVM classifier shown against average rainfall amount in the study area

where managers can apply restrictions on access to irrigation water (Lionboui et al. 2016).

As a result, they give priority to the maintenance of orchards without a production goal and limit the areas of annual crops. This is reflected in the stability of the perennial crops superficies, unlike annual crops superficies that regress (Fig. 8). Farmers in the study area practice supplementary irrigation. During a dry year, the farmer using pumping as the main source of irrigation will abandon his land or give up cultivation given the very high energy cost. This implies a reduction in the superficies of the irrigated annual crops by pumping. This is the case of 2015/2016 cropping season with an average of rainfall amount of 128 mm and a superficies of 534,081 ha. Adversely, cropping seasons with an average rainfall amount higher than 370 mm, e.g., 2014/2015 cropping season, reach superficies greater than 580,890 ha (Fig. 8).

Although, the classification of agricultural systems based on phenological parameters as an input of the classification algorithm meets the objective to map the main phenological classes at large scale (Fig. 7). This approach based on the low spatial resolution data can be seen as a preliminary step before moving on to higher resolution products.

Over inter-annual time scales, phenological patterns of rainfed crop areas depend strongly on the spatio-temporal fluctuations of rainfall and dry periods. Therefore, the phenological analysis provides information to deepen our understanding about the spatio-temporal variability of land surface phenology in arid and semi-arid area on one hand, and on the other, to improve agricultural system monitoring that allows managers and policy makers to optimize the agricultural vocation and land suitability. These fluctuations in rainfall amount have a negative impact on agricultural systems, especially in arid and semi-arid region like the soil degradation (e.g., soil salinity, nutrient depletion) and the quality and depth of groundwater. Furthermore, the proportion of groundwater used for irrigation of croplands increases in parallel with the overall decline in rainfall, which decreases the groundwater amount and leads to the degradation of croplands.

## 4 Conclusion

This study examines the use of remote sensing data to characterize and map the spatio-temporal phenological metrics variability through Beni-Mellal-Khenifra region between 2012 and 2016. Phenology-based classification approach showed a high ability to identify and monitor the main agricultural system in the study area. The classification overall accuracy reached 88%, with a kappa coefficient of 0.83. The F1-score values for all classes were greater than 0.76. Analyzing the results, the rainfed area shows a dependence on the spatio-temporal fluctuations of rainfall, this result can be extended in further studies on the characterization of drought in agricultural zones. Therefore, the phenological analysis provides information to deepen our understanding of the spatio-temporal variability of land surface phenology in arid and semi-arid area. In perspective, assessment of environmental, agronomic and socio-economic consequences of phenological changes can improve the awareness of stakeholders to adapt it to take decisions to limit the impacts of change on ecosystems and society. The results demonstrated the ability of phenological parameters to identify and monitor the main agricultural system classes in the study area and to control the illegal pumping zones and the irrigated area.

**Acknowledgements** The authors are grateful to NASA's team, for creating and making the vegetation index product MOD13Q1 freely available. We also would like to thank Pr. Eklundh and his team for their available help on TIMESAT software.

## Compliance with Ethical Standards

**Conflict of interest** The authors declare no conflict of interest.

## References

Alcantara C, Kuemmerle T, Prishchepov AV, Radeloff VC (2012) Mapping abandoned agriculture with multi-temporal MODIS satellite data. Remote Sens Environ 124:334–347. https://doi.org/10.1016/j.rse.2012.05.019

Almazroui M, Islam MN, Balkhair KS, Şen Z, Masood A (2017a) Rainwater harvesting possibility under climate change: a basin-scale case study over western province of Saudi Arabia. Atmos Res 189:11–23. https://doi.org/10.1016/j.atmosres.2017.01.004

Almazroui M, Nazrul Islam M, Saeed S, Alkhalaf AK, Dambul R (2017b) Assessment of Uncertainties in projected temperature and precipitation over the Arabian Peninsula using three categories of Cmip5 multimodel ensembles. Earth Syst Environ 1:23. https://doi.org/10.1007/s41748-017-0027-5

Arvor D, Jonathan M, Meirelles M, Dubreuil V, Durieux L (2011) Classification of MODIS EVI time series for crop mapping in the state of Mato Grosso. Brazil Int J Remote Sens 32:7847–7871. https://doi.org/10.1080/01431161.2010.531783

Bachoo A, Archibald S (2007) Influence of using date-specific values when extracting phenological metrics from 8-day composite NDVI data. In: 2007 international workshop on the analysis of multi-temporal remote sensing images, 18–20 July 2007, pp 1–4. https://doi.org/10.1109/multitemp.2007.4293044

Barakat A, Ouargaf Z, Khellouk R, El Jazouli A, Touhami F (2019) Land use/land cover change and environmental impact assessment in Béni-Mellal District (Morocco) using remote sensing and GIS. Earth Syst Environ 3:113–125. https://doi.org/10.1007/s41748-019-00088-y

Benabdelouahab T, Balaghi R, Hadria R, Lionboui H, Minet J, Tychon B (2015) Monitoring surface water content using visible and short-wave infrared SPOT-5 data of wheat plots in irrigated semi-arid regions. Int J Remote Sens 36:4018–4036. https://doi.org/10.1080/01431161.2015.1072650

Benabdelouahab T, Balaghi R, Hadria R, Lionboui H, Djaby B, Tychon B (2016) Testing aquacrop to simulate durum wheat yield and schedule irrigation in a semi-arid irrigated perimeter in Morocco. Irrig Drain 65:631–643. https://doi.org/10.1002/ird.1977

Biggs TW, Thenkabail PS, Gumma MK, Scott CA, Parthasaradhi GR, Turral HN (2006) Irrigated area mapping in heterogeneous landscapes with MODIS time series, ground truth and census data, Krishna Basin, India. Int J Remote Sens 27:4245–4266. https://doi.org/10.1080/01431160600851801

Boschetti M, Stroppiana D, Brivio PA, Bocchi S (2009) Multi-year monitoring of rice crop phenology through time series analysis of MODIS images. Int J Remote Sens 30:4643–4662. https://doi.org/10.1080/01431160802632249

Chen J, Jönsson P, Tamura M, Gu Z, Matsushita B, Eklundh L (2004) A simple method for reconstructing a high-quality NDVI time-series data set based on the Savitzky–Golay filter. Remote Sens Environ 91:332–344. https://doi.org/10.1016/j.rse.2004.03.014

Chen JL, Wilson CR, Seo KW (2006) Optimized smoothing of Gravity Recovery and Climate Experiment (GRACE) time-variable gravity observations. J Geophys Res Solid Earth 1:1. https://doi.org/10.1029/2005jb004064

CRI (2015) Centre Régional d'Investissement-Béni Mellal khénifra, Monographie de la région de Béni Mellal-Khénifra, Octobre 2015

DeFries RS, Field CB, Fung I, Collatz GJ, Bounoua L (1999) Combining satellite data and biogeochemical models to estimate global effects of human-induced land cover change on carbon emissions and primary productivity. Glob Biogeochem Cycles 13:803–815. https://doi.org/10.1029/1999GB900037

Didan K (2015) MOD13Q1 MODIS/Terra Vegetation Indices 16-Day L3 Global 250 m SIN Grid V006. NASA EOSDIS Land Processes DAAC. https://doi.org/10.5067/modis/mod13q1.006

Diouf AA, Djaby B, Diop MB, Wele A, Ndione JA, Tychon B (2014) Fonction d'ajustement pour l'estimation de la production fourragère herbacée des parcours naturels du Sénégal à partir du NDVI S10 de SPOT-VEGETATION. In: XXVIIe Colloque de l'Association Internationale de Climatologie, Dijon, France

Diouf AA, Faye G, Minet J, Djaby B, Ndione JA, Tychon B (2015) Zonage phénoclimatique et caractérisation des parcours naturels du sénégal avec les données de télédétection satellitaire. In: XXVIIIe Colloque de l'Association Internationale de Climatologie, Liège, Bélgique

Dixon RK, Solomon AM, Brown S, Houghton RA, Trexier MC, Wisniewski J (1994) Carbon pools and flux of global forest ecosystems. Science 263(5144):185–190

Eklundh L, Jönsson P (2015) Timesat 3.2 software manual. Lund and Malmö University, Sweden

Evrendilek F, Gulbeyaz O (2011) Boosted decision tree classifications of land cover over Turkey integrating MODIS, climate and topographic data. Int J Remote Sens 32:3461–3483. https://doi.org/10.1080/01431161003749469

Geng L, Ma M, Wang X, Yu W, Jia S, Wang H (2014) Comparison of eight techniques for reconstructing multi-satellite sensor time-series NDVI Data Sets in the Heihe River Basin. China Remote Sens 6:2024

Hadria R et al (2006) Monitoring of irrigated wheat in a semi-arid climate using crop modelling and remote sensing data: impact of satellite revisit time frequency. Int J Remote Sens 27:1093–1117. https://doi.org/10.1080/01431160500382980

Hadria R, Khabba S, Lahrouni A, Duchemin B, Chehbouni A, Carriou J, Ouzine L (2007) Calibration and validation of the STICS crop model for managing wheat irrigation in the semi-arid Marrakech/Al Haouz Plain. Arab J Sci Eng 32:87–101

Hadria R, Benabdelouahab T, Mahyou H, Balaghi R, Bydekerke L, El Hairech T, Ceccato P (2018) Relationships between the three components of air temperature and remotely sensed land surface temperature of agricultural areas in Morocco. Int J Remote Sens 39:356–373. https://doi.org/10.1080/01431161.2017.1385108

Jed Wing MKC et al (2018) Caret: classification and regression training

Ji L, Peters AJ (2007) Performance evaluation of spectral vegetation indices using a statistical sensitivity function. Remote Sens Environ 106:59–65. https://doi.org/10.1016/j.rse.2006.07.010

Jönsson P, Eklundh L (2002) Seasonality extraction by function fitting to time-series of satellite sensor data. IEEE Trans Geosci Remote Sens 40:1824–1832

Jönsson P, Eklundh L (2004) TIMESAT a program for analyzing time-series of satellite sensor data. Comput Geosci 30:833–845. https://doi.org/10.1016/j.cageo.2004.05.006

Jung M, Henkel K, Herold M, Churkina G (2006) Exploiting synergies of global land cover products for carbon cycle modeling. Remote Sens Environ 101:534–553. https://doi.org/10.1016/j.rse.2006.01.020

Kaptué A, Roujean J-L, De Jong SM (2011) Comparison and relative quality assessment of the GLC2000, GLOBCOVER, MODIS and ECOCLIMAP land cover data sets at the African continental scale. Int J Appl Earth Obs Geoinf 13:207–219. https://doi.org/10.1016/j.jag.2010.11.005

Lambin EF, Turner BL, Helmut JG et al (2001) The causes of land-use and land-cover change: moving beyond the myths. Glob Environ Change 11:261–269

Lessel J, Ceccato P (2016) Creating a basic customizable framework for crop detection using Landsat imagery. Int J Remote Sens 37:6097–6107. https://doi.org/10.1080/2150704X.2016.1252471

Lieth H (1974) Phenology and seasonality modeling, vol 8. Springer, New York

Lionboui H, Fadlaoui A, Elame F, Benabdelouahab T (2014) Water pricing impact on the economic valuation of water resources. Int J Educ Res 2:147

Lionboui H, Benabdelouahab T, Elame F, Hasib A, Boulli A (2016) Multi-year agro-economic modelling for predicting changes in irrigation water management indicators in the Tadla sub-basin. Int J Agric Manag 5:96–105. https://doi.org/10.5836/ijam/2016-05-96

Löw F, Michel U, Dech S, Conrad C (2013) Impact of feature selection on the accuracy and spatial uncertainty of per-field crop classification using Support Vector Machines. ISPRS J Photogramm Remote Sens 85:102–119. https://doi.org/10.1016/j.isprsjprs.2013.08.007

Marchane A et al (2015) Assessment of daily MODIS snow cover products to monitor snow cover dynamics over the Moroccan Atlas mountain range. Remote Sens Environ 160:72–86. https://doi.org/10.1016/j.rse.2015.01.002

Matsushita B, Yang W, Chen J, Onda Y, Qiu G (2007) Sensitivity of the enhanced vegetation index (EVI) and normalized difference vegetation index (NDVI) to topographic effects: a case study in high-density cypress forest. Sensors (Basel, Switzerland) 7:2636–2651

McGill R, Tukey JW, Larsen WA (1978) Variations of box plots. Am Stat 32:12–16. https://doi.org/10.1080/00031305.1978.10479236

McVicar TR, Jupp DLB (1998) The current and potential operational uses of remote sensing to aid decisions on drought exceptional circumstances in Australia: a review. Agric Syst 57:399–468. https://doi.org/10.1016/S0308-521X(98)00026-2

Mottaleb KA, Gumma MK, Mishra AK, Mohanty S (2015) Quantifying production losses due to drought and submergence of rainfed rice at the household level using remotely sensed MODIS data. Agric Syst 137:227–235. https://doi.org/10.1016/j.agsy.2014.08.014

Mountrakis G, Im J, Ogole C (2011) Support vector machines in remote sensing: a review. ISPRS J Photogram Remote Sens 66:247–259. https://doi.org/10.1016/j.isprsjprs.2010.11.001

NASA LP DAAC 2017, MOD13Q1. Version 6. NASA EOSDIS Land Processes DAAC, USGS Earth Resources Observation and Science (EROS) Center, Sioux Falls, South Dakota (https://lpdaac.usgs.gov). Accessed 13 Apr 2017. http://dx.doi.org/10.5067/MODIS/MOD13Q1.006

Ouatiki H et al (2017) Evaluation of TRMM 3B42 V7 rainfall product over the Oum Er Rbia watershed in Morocco. Climate 5:1

Ouatiki H, Boudhar A, Ouhinou A, Arioua A, Hssaisoune M, Bouamri H, Benabdelouahab T (2019) Trend analysis of rainfall and drought over the Oum Er-Rbia River Basin in Morocco during 1970–2010. Arab J Geosci 12:128. https://doi.org/10.1007/s12517-019-4300-9

Pal M, Mather PM (2005) Support vector machines for classification in remote sensing. Int J Remote Sens 26:1007–1011. https://doi.org/10.1080/01431160512331314083

Peng J, Dan L, Dong W (2009) Estimate of extended long-term LAI data set derived from AVHRR and MODIS based on the correlations between LAI and key variables of the climate system from 1982 to 2009. Int J Remote Sens 34:7761–7778. https://doi.org/10.1080/01431161.2013.826840

R Core Team (2017) R: a language and environment for statistical computing

Reed BC, Brown Jesslyn F, VanderZee D, Loveland TR, Merchant JW, Ohlen DO (1994) Measuring phenological variability from satellite imagery. J Veg Sci 5:703–714

René A, Nathalie R (2007) L'agriculture du Maghreb au défi du changement climatique: Quelles stratégies d'adaptation face à la raréfaction des ressources hydriques? Paper presented at the WATMED 3,3e conférence internationale sur les Ressources en Eau dans le Bassin Méditerranéen <halshs-00134115>, Tripoli 1–3 novembre 2006

Schmidt M, Lucas R, Bunting P, Verbesselt J, Armston J (2015) Multi-resolution time series imagery for forest disturbance and regrowth monitoring in Queensland. Aust Remote Sens Environ 158:156–168. https://doi.org/10.1016/j.rse.2014.11.015

Schwartz MD (2003) Phenology: an integrative environmental science. Tasks for vegetation science, vol 39. Kluwer Academic Publishers, Dordrecht

Shahriar PM, Budde M, Rowland J (2014) Mapping irrigated areas in Afghanistan over the past decade using MODIS NDVI. Remote Sens Environ 149:155–165. https://doi.org/10.1016/j.rse.2014.04.008

Shao Y, Lunetta RS (2012) Comparison of support vector machine, neural network, and CART algorithms for the land-cover classification using limited training data points. ISPRS J Photogram Remote Sens 70:78–87. https://doi.org/10.1016/j.isprsjprs.2012.04.001

Sun H, Xu A, Lin H, Zhang L, Mei Y (2012) Winter wheat mapping using temporal signatures of MODIS vegetation index data. Int J Remote Sens 33:5026–5042. https://doi.org/10.1080/01431161.2012.657366

Tucker CJ, Vanpraet C, Boerwinkel E, Gaston A (1983) Satellite remote sensing of total dry matter production in the Senegalese Sahel. Remote Sens Environ 13:461–474

Vapnik VN (2006) Estimation of dependence based on empirical data: empirical inference science afterword of 2006. Information science and statistics. Springer, New York. https://doi.org/10.1007/0-387-34239-7

Viña A, Gitelson AA, Rundquist DC, Keydan G, Leavitt B, Schepers J (2004) Monitoring maize (*Zea mays* L.) phenology with remote sensing. Agron J 96:1139–1147. https://doi.org/10.2134/agronj2004.1139

Vrieling A, de Beurs KM, Brown ME (2011) Variability of African farming systems from phenological analysis of NDVI time series. Clim Change 109:455–477. https://doi.org/10.1007/s10584-011-0049-1

Wardlow B, Egbert S, Kastens J (2007) Analysis of time-series MODIS 250 m vegetation index data for crop classification in the U.S. Central Great Plains. Remote Sens Environ 108:290–310. https://doi.org/10.1016/j.rse.2006.11.021

Winkler K, Gessner U, Hochschild V (2017) Identifying droughts affecting agriculture in Africa based on remote sensing time series between 2000–2016: rainfall anomalies and vegetation condition in the context of ENSO. Remote Sens 9:831

Wu D, Qu JJ, Hao X (2015) Agricultural drought monitoring using MODIS-based drought indices over the USA Corn Belt. Int J Remote Sens 36:5403–5425. https://doi.org/10.1080/01431161.2015.1093190

Zhao Q, Brocks S, Lenz-Wiedemann VIS, Miao Y, Zhang F, Bareth G (2017) Detecting spatial variability of paddy rice yield by combining the DNDC model with high resolution satellite images. Agric Syst 152:47–57. https://doi.org/10.1016/j.agsy.2016.11.011